

Design and Performance Analysis of a Novel Rotary Transformer for Brushless Application

Hui Zhong¹, Chao Wu¹, Yubo Yang¹

¹Shandong University, 17923 Jingshi Road, Jinan, Shandong, 250061, China, zhonghui@sdu.edu.cn

This paper presents a novel rotary transformer for power supplying rotatable parts of electrical applications as a robust alternative to sliding contacts. To get the accurate parameters of the proposed transformer, two kinds of transformer model, the classical ideal transformer model and the UMEC (Unified Magnetic Equivalent Circuit) model, are derived. The influence of the geometry design parameters of the rotary transformer on its performance is discussed by 3-D Finite Element Analysis method. The 3-D flux density vector is calculated by the electromagnetic field analysis, including the core end regions. Based on the results, a resonant circuit is selected to be combined with the transformer considering both the transfer efficiency and a doubly fed induction generator performance. The finite-element analysis and experimental results are used to verify the obtained analytical model.

Index Terms—Electromagnetic coupling, magnetic reluctance circuit, rotary transformer, 3-D finite element analysis

I. INTRODUCTION

IT is necessary to transmit electrical power from a stationary source to a rotating load or circuit in many industrial applications such as wound-rotor synchronous^[1], doubly fed induction generator^[2-4], radar power supplies^[5] and so on. Although using of the brushed equipments is a simple, compact and low-cost solution, the presence of brushes and slip rings increases the maintenance costs and limits the machine only to non-explosive environments due to the mechanical wearing. To make a contactless maintenance-free solution, different brushless structures are proposed. This paper presents a novel rotary transformer for power supplying rotatable parts of electrical applications as a robust alternative to sliding contacts. The finite-element analysis and simulation results are used to verify the obtained analytical model

II. ROTARY TRANSFORMER

An example for a three phases rotary transformer application in can be found in [2]. One phase structure of the proposed rotary transformer is shown in Fig.1, which indicating the position of the stator, the rotor and the windings.. The inner part (secondary side) of the transformer moves with the generator rotor. The outer part (primary side) stands still.

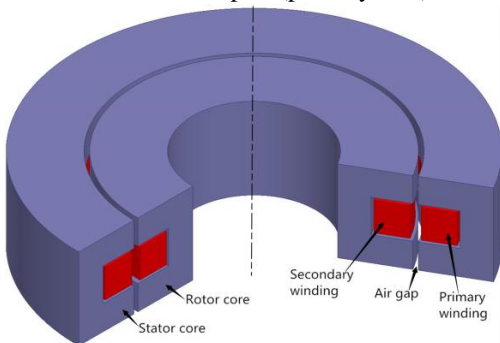


Fig. 1. Structure of one phase rotary transformer core

The operational principle of the rotary transformer is the same as the ones of the general static transformer. The ratio of induction electromotive force of the primary and secondary

windings is equal to the ones of the turns of the primary and secondary windings.

$$V_p / V_s = N_p / N_s, \quad (1)$$

Where V_p and V_s are the primary and secondary winding induction electromotive force of the transformer, N_p and N_s are the corresponding equivalent turn numbers.

III. ELECTROMAGNETIC DESIGN

A. Constructive constraints and design.

One design challenge of the rotary transformer is the air gap of radial freedom to allow a small axial movement without affecting the electrical characteristics too much. The possible designs are limited by the constructive constraints such as the axial length l_{ax} , the outer diameter d_{out} , the desired air gap length c or the rotational speed n . The detail of the constructive parameters and cross section of the rotary transformer will be shown in the full paper.

B. Optimization.

Based on the single-objective genetic algorithm, the main dimensions of the rotary transformer are optimized.

IV. MAGNETIC MODEL

To get the accurate parameters of the proposed transformer, the classical model and the unified magnetic equivalent circuit (UMEC) model of the transformers are summarized and derived.

A. Classical model

The classical model is divided into ideal transformer model and the model basing on controlled source principle.

B. UMEC model

The advantages of the UMEC model such as needing no winding turns, core cross-sectional area and the length and so on, as well as the relationship between core permeance and yoke permeance, are fully utilized by the model, so that the non-linearization of the yoke can also be indirectly considered.

The model is shown in Fig. 2. The magnetizing inductance is calculated by

$$L_m = N_p^2 / [R_{cp1} + R_{cp2} + R_{cp3} + R_{cs1} + R_{cs2} + R_{cs3} + R_{ag1} + R_{ag2}] \quad (2)$$

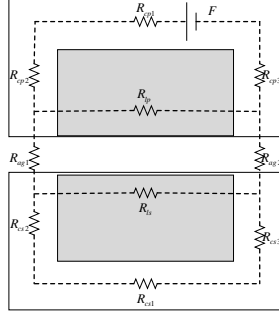


Fig.2. UMEC model of the rotating transformer.

By using energy approach, an expression of the total leakage inductance of the transformer which is seen from the primary side are as follows

$$L_{lk} = \mu_0 N_p^2 \frac{MLT}{a} \left(c + \frac{b_1 + b_2}{3} \right) \quad (3)$$

Where, MLT presents the mean length turn of the volume (coil and air gap).

C. Finite element model

In order to describe the magnetic behavior of the rotary transformer, a 3-D finite element model is built to calculate the flux density in the air gap and cores. An efficient method(alternating flux linkage method) is introduced to speed up the transient process for fast reaching the AC steady state. The DC flux linkage is eliminated by applying an additional voltage component within a small time interval^[6]. The flux linkages at the end of this interval are the perfect initial values for flux linkages in the successive transient simulation. As a result, the steady-state AC flux linkages can be obtained immediately within the next period. In transient FEA solvers, the initial field solution can be obtained via static field analysis based on the initial winding currents. After the DC component of the flux linkage decays to zero, the flux linkage will reach the steady state value. If the applied voltage is modified in such a way that the DC component of the flux linkage is zero after time t_s , the steady state can be immediately reached for $t > t_s$.

The flux linkage for $t > t_s$ is:

$$\begin{aligned} \psi(t) &= \psi(0) + \int_0^t [u(t) + u_d(t)] dt \\ &= -\psi_m \cos(\omega t + \varphi) + \psi(0) + \psi_m \cos \varphi + \int_0^t \Delta u(t) dt \end{aligned} \quad (4)$$

In (4), $u(t)$ can be any function and t_s can be freely selected.

As long as $\int_0^t \Delta u(t) dt = -[\psi(0) + \psi_m \cos \varphi]$, the DC component of the flux linkage at t_s will be zero, and the flux linkage will reach the steady state after time t_s . One possible select is:

$$\begin{cases} t_s = T/2 \\ \Delta u(t) = U_{dm} \sin(\omega t) \end{cases} \quad (5)$$

The results show that leakage flux strongly influences the flux with a considerable effect on the magnetic field in this transformer, as presented in Fig. 3.

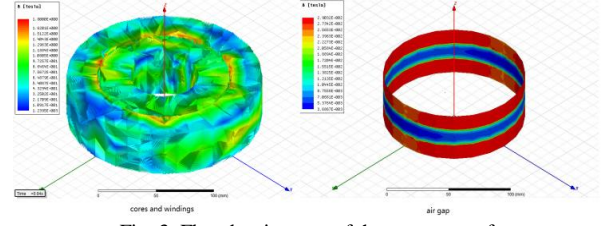


Fig. 3. Flux density map of the rotary transformer

The magnetic flux density amplitude of the air gap in one cycle is shown in Fig.4

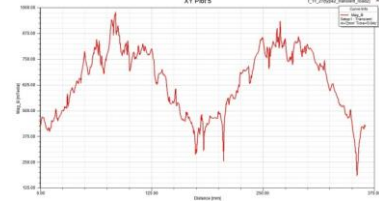


Fig. 4. Magnetic flux density amplitude of the air gap at time=0.04s

V. VERIFICATION WITH A DOUBLE -FED GENERATOR

The validity of the proposed rotary transformer is verified by a high speed double-fed induction generator. The generator applies two three-phase high frequency inverters connected to stator and rotor windings in order to realize high speed operation. The most common way to access the rotor winding is using slip rings and brushes. To resolve the wear-out and spark problems, the rotary transformer is proposed to replace the slip rings and brushes.

The resonant capacitors which are placed in series on both sides of the transformer are used to improve the power transformer. The finite element simulation result is normalized to compare with the theoretical result and equivalent circuit analyses. The details will be talked in full paper.

ACKNOWLEDGMENT

The work has been supported by National Natural Science Foundation of China (NSFC) under grant #51307100.

REFERENCES

- [1] Patin, N., Monmasson, E., Louis, J.P.: "Modeling and control of a cascaded doubly fed induction generator dedicated to isolated grid," IEEE Trans. Ind. Electron., 2009, 56, (10), pp. 4207–4219
- [2] H. Zhong, L. Zhao, and X. Li, "Design and analysis of a three-phase rotary transformer for doubly fed induction generators," IEEE Trans. Ind. Appl., vol. 51, no. 4, pp. 2791–2796, Jul./Aug. 2015
- [3] M. Ruviaro and F. Runcos, "Analysis and test results of a brushless doubly fed induction machine with rotary transformer," IEEE Trans. Ind. Electron., vol. 59, no. 6, pp. 2670–2677, Jun. 2012.
- [4] M. Ruviaro, F. Runcos, and N. Sadowski, "Wound Rotor Doubly Fed Induction Machine with Radial Rotary Transformer," Journal of Microwaves, Optoelectronics and Electromagnetics Applications, vol. 12, no. 2, pp. 1–16, 2013.
- [5] K. D. Papastergiou and D. E. Macpherson, "An airborne radar power supply with contactless transfer of energy—Part I: Rotating transformer," IEEE Trans. Ind. Electron., vol. 54, no. 5, pp. 2874–2884, Oct. 2007.
- [6] S. A. Mousavi, C. Carrander, and G. Engdahl, "Comprehensive study on magnetization current harmonics of power transformers due to GICs," in International Conference on Power Systems Transients (IPST 2013), Vancouver, Canada, July 18-20, 2013